Supporting Information

In situ electrochemical activation of Ni-based colloids from $NiCl_2$ electrode and their advanced energy storage performance

*Kunfeng Chen, and Dongfeng Xue**

State Key Laboratory of Rare Earth Resource Utilization, Changchun Institute of Applied Chemistry, Chinese Academy of Sciences, Changchun 130022, China.
E-mail: dongfeng@ciac.ac.cn

Experimental Section

Electrode preparation: In this work, no complex synthesis method was needed and the $NiCl_2{\cdot}6H_2O$ salts were directly used as electroactive materials. Firstly, Ni salt ($NiCl_2{\cdot}6H_2O$), carbon black, and polyvinylidene fluoride (PVDF) in a mass ratio of 60:30:10 were mixed with N-methyl-2-pyrrolidone (NMP) to obtain slurry. Then, the resulting slurry was pasted onto nickel foam current collector ($1cm^2$) and dried at 80°C for 24 h. Then, the sheet of nickel foam with Ni salt was pressed at 10 MPa and this served as working electrode. The electrode loading of $NiCl_2{\cdot}6H_2O$ was between 2 and 3 mg for each electrode.

In-situ materials synthesis: In situ electrochemical synthesis was performed in a three-electrode cell, in which the saturated calomel electrode (SCE) and Pt wire were used as the reference and counter electrodes. The electrolyte used was 2 M KOH solution. Cyclic voltammetry (CV) method was used to run in situ electrochemical reaction to synthesize electroactive materials. The scan rate was 50mV/s and the potential range used was 0-0.45 V vs. SCE. After CV testing for 50 cycles, electroactive working electrode was obtained with active materials within the electrode. These electrodes were used for further characterization and electrochemical measurement.

Electrochemical performance testing: After in-situ materials synthesis, the electroactive working electrode was directly used for supercapacitor. Electrochemical performance testing, such as CV, galvanostatic charge-discharge and electrochemical impedance spectroscopy measurements were performed in the same electrolyte. An electrochemical workstation (CHI 660D) was used to run these electrochemical experiments in a three-electrode configuration at room temperature.

Specific capacitance C_s values can be calculated through integration, as expressed by the following equation:

$$C_s = \frac{2I \cdot \int V dt}{m \cdot \Delta V^2} \tag{1}$$

where I is the discharge current, dt is the discharge time, m is the mass of Ni^{2+}, and ΔV is the potential interval. The specific capacitance C_s can be approximately calculated using the following equation: $C_s = I\Delta t/m\Delta V$, where I is the discharge current, Δt is the discharge time, m is the mass of Ni^{2+} in g, and ΔV is the potential interval.

***Asymmetric supercapacitor device*:** For the fabrication of asymmetric supercapacitor, an activated carbon electrode (negative electrode) was prepared by mixing 80 wt% activated carbon and 10 wt% PVDF to obtain slurry. Then the slurry was cast onto a 1 cm^2 nickel foam and dried at 80°C for 24 h. The activated carbon electrode was combined with a $NiCl_2$ electrode (positive electrode) with one piece of cellulose paper as the separator and 2 M KOH as the electrolyte to assemble the full cell. The energy density was calculated using equation $E = CV^2/2$, where C is the specific capacitance, V is the potential interval of the discharge. The average power density during discharge was calculated according to the equation, $P = E/t$ (W/g), where t (h) is the discharge time. All electrochemical measurements were run by a CHI 660D electrochemical workstation.

***Characterization*:** The crystalline phases of the materials were determined by powder X-ray diffraction with Cu Kα radiation (λ = 0.15418 nm) on a Bruker D8 Focus diffractometer. Infrared (IR) spectral studies were carried out by ATR-IR technique (Thermo Nexus 6700) with an ATR cell and the internal reflection element (IRE) was diamond crystal. The microstructure of the electrode samples was characterized by field-emission scanning electron microscope (FESEM, Hitachi-S4800), and transmission electron microscope (TEM, FEI Tecnai G2 F20).

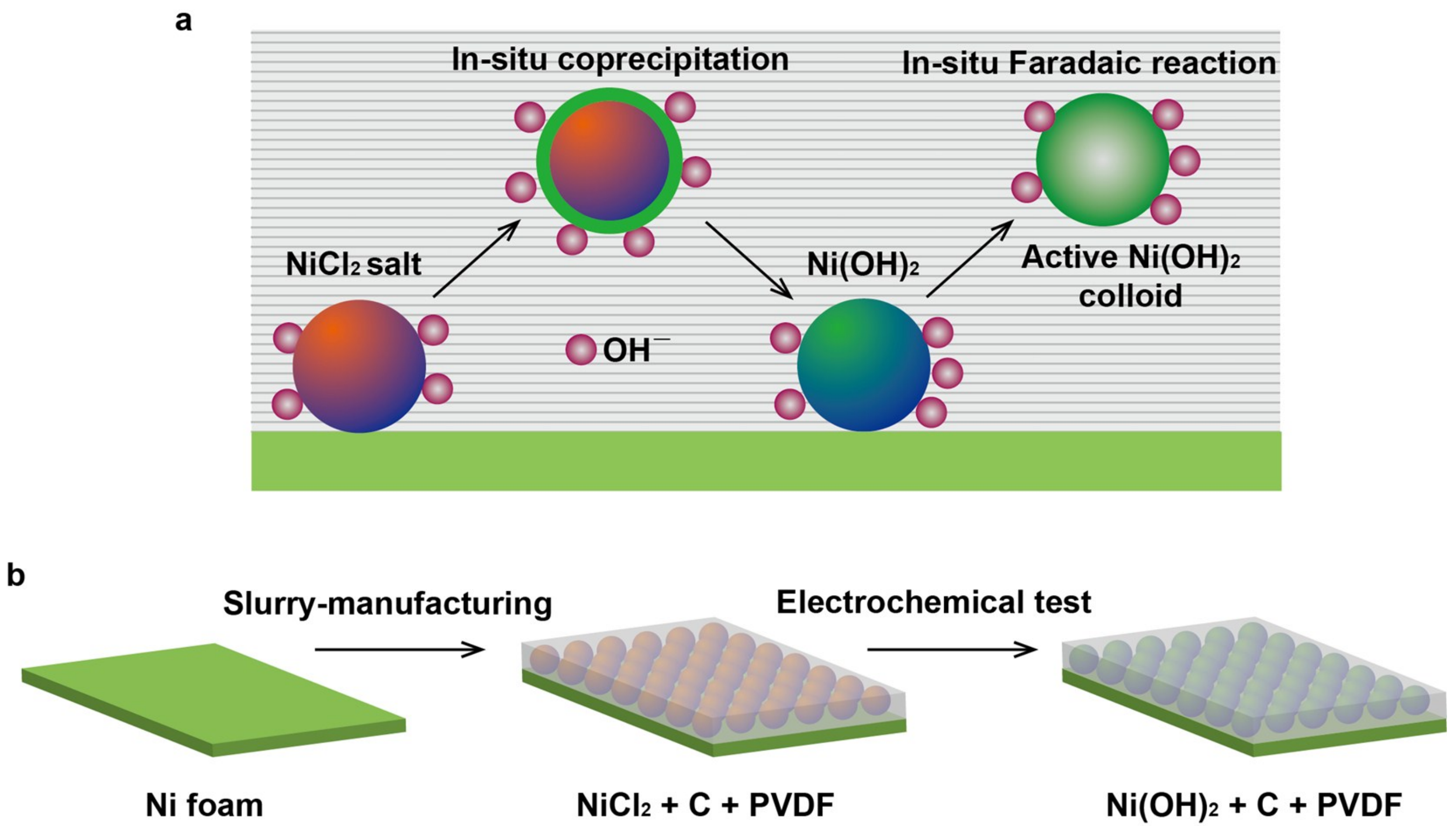

Figure S1. Schematic illustration shows the assembly of alkaline $NiCl_2$ supercapacitors. (a) The formation of highly electroactive $Ni(OH)_2$ colloids by in-situ chemical coprecipitation and in-situ Faradaic reaction. (b) The fabrication of $NiCl_2{\cdot}6H_2O$ salt electrode by two-step: (1) slurry-manufacturing and (2) in-situ electrochemical reaction. Both the chemical reaction and electrochemical reaction occurred simultaneously at the same electrode. The $Ni(OH)_2$ colloid can be completely utilized to deliver the high specific capacitance.

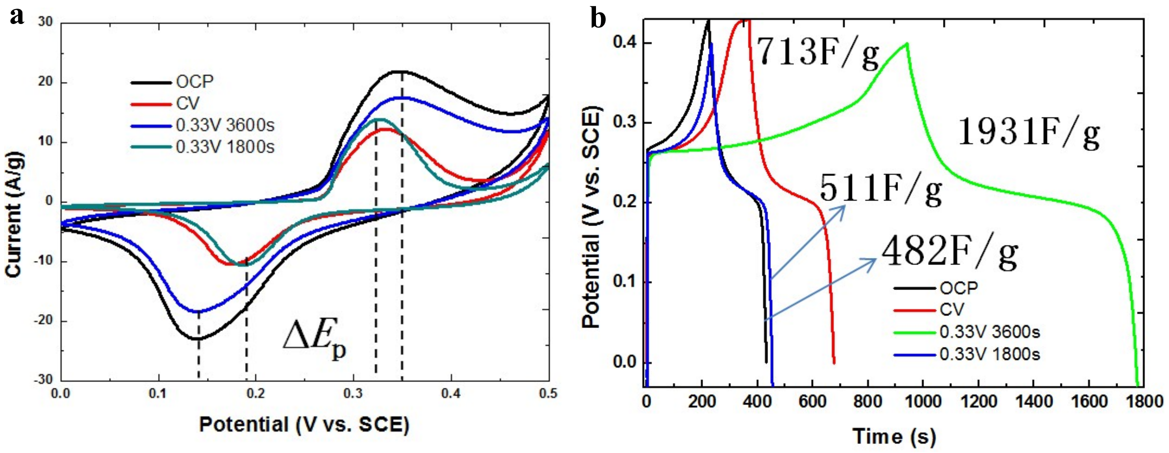

Figure S2. Electrochemical responses of different activation methods. (a) CV curves at 10 mV/s, (b) charge-discharge curves at 1A/g.

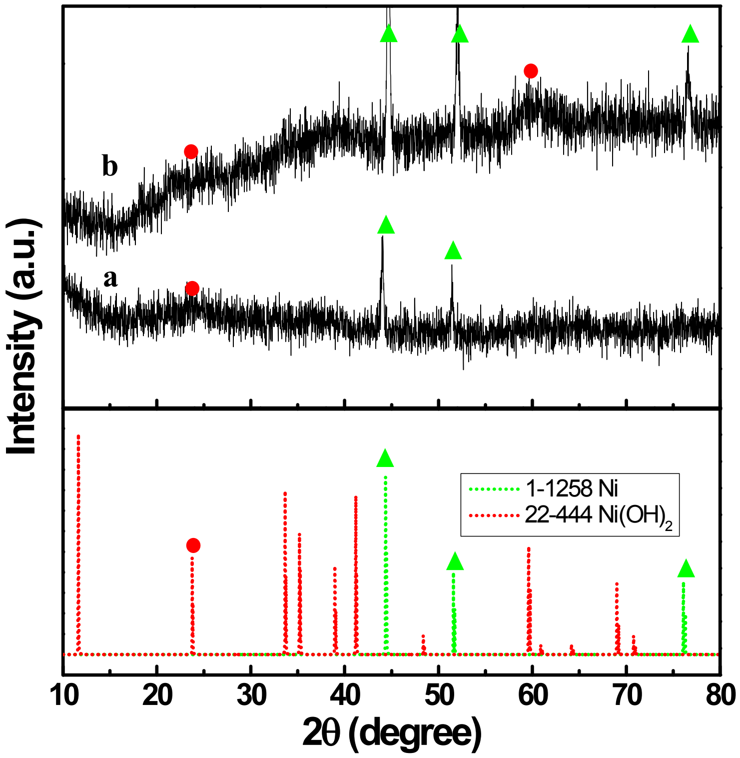

Figure S3. XRD patterns of $NiCl_2$ salt supercapacitors after electrochemical measurements with the standard No. JCPDS No. 22-444 for α-$Ni(OH)_2$. (a) $NiCl_2$ salt electrode including Ni salt and carbon without adding binder, (b) $NiCl_2$ salt electrode only including Ni salt without adding binder and conducting carbon. Both of the electrodes include α-$Ni(OH)_2$. The peaks of Ni current collector were also indicated in the figures with the standard No. JCPDS No. 1-1258.

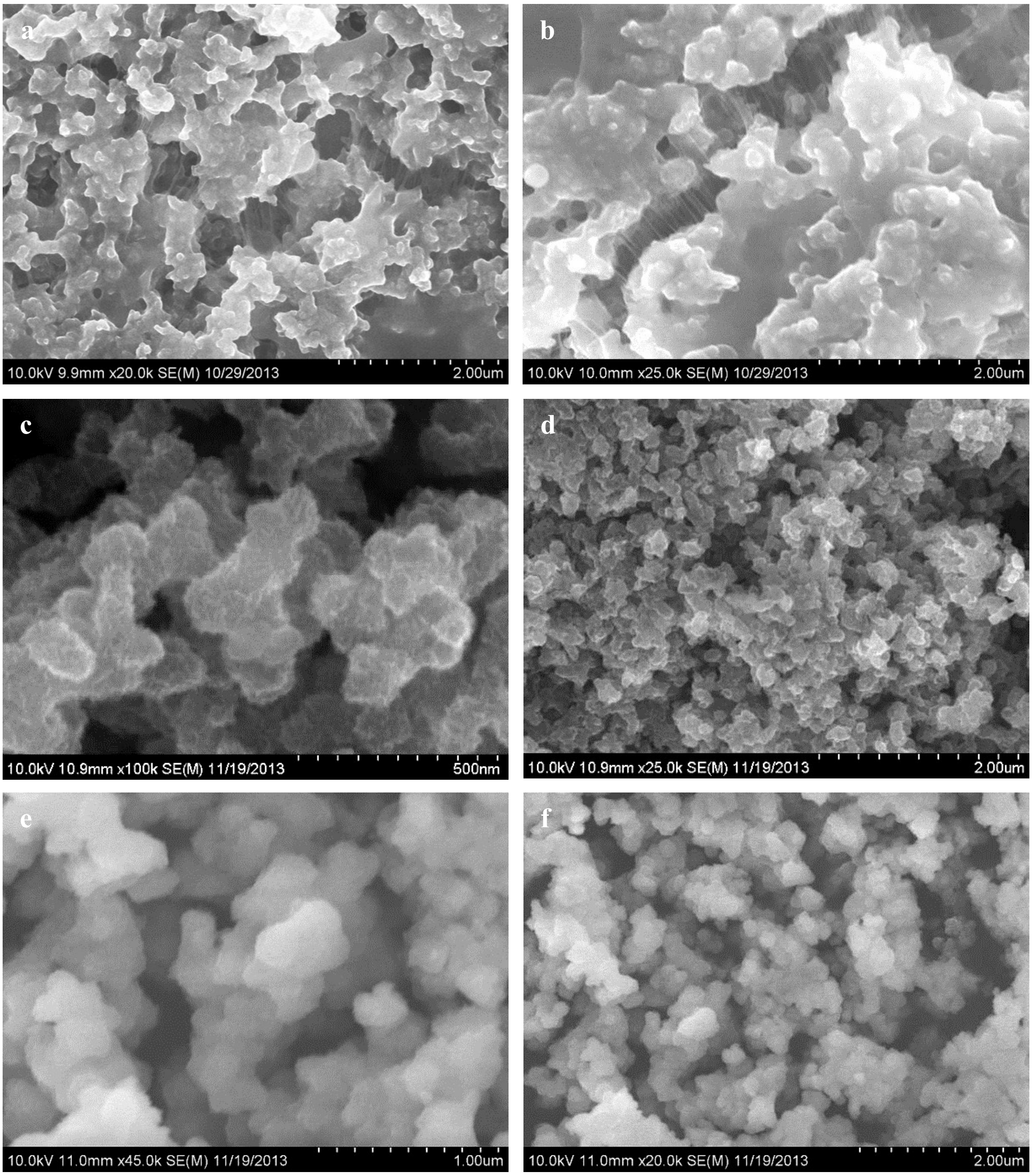

Figure S4. SEM images of $NiCl_2$ salt supercapacitors after electrochemical measurements: (a, b) $NiCl_2$ salt electrode including Ni salt, binder and conducting carbon. (c, d) $NiCl_2$ salt electrode including Ni salt and carbon without adding binder, (e, f) $NiCl_2$ salt electrode only including Ni salt without adding binder and conducting carbon.

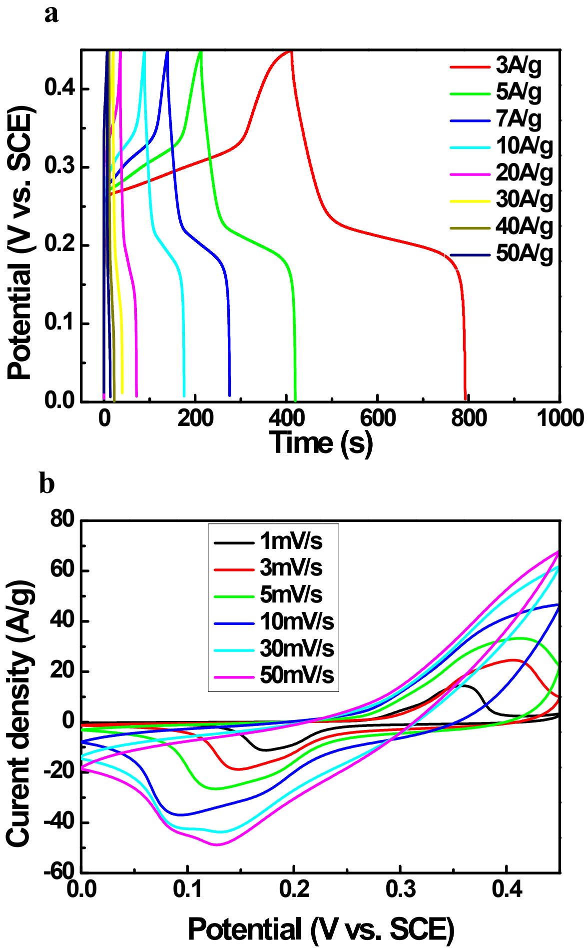

Figure S5 Electrochemical performance of $NiCl_2$ supercapacitor. (a) The charge-discharge curves (time versus potential) measured at various current densities and potential range of 0-0.45 V, and (b) CV curves (current density versus potential) obtained at potential range of 0-0.45 V with various scan rates. All data were collected in a 2 M KOH solution at room temperature.

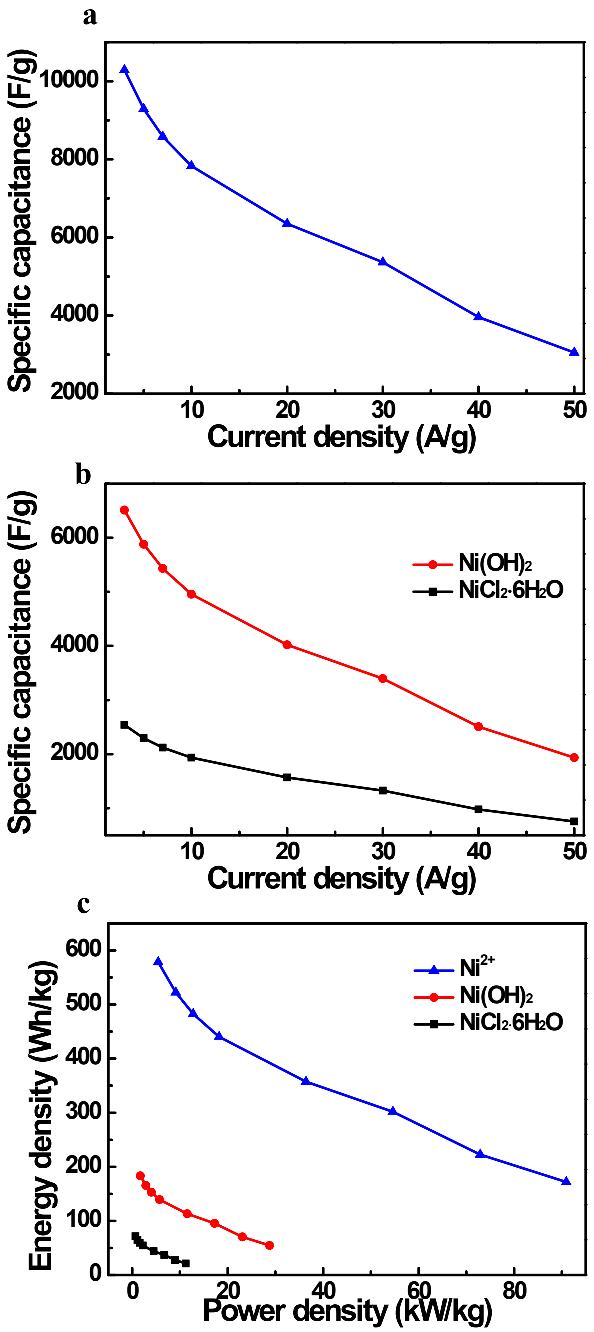

Figure S6 The specific capacitance versus the current density normalized to the weight of Ni^{2+} ion (a) and the weight of $Ni(OH)_2$ and $NiCl_2 \cdot 6H_2O$ (b). (c)The energy density as a function of the power density normalized to the weight of Ni^{2+} ion, $Ni(OH)_2$ and $NiCl_2 \cdot 6H_2O$.

Table S1 Pseudocapacitance of Ni^{2+} cations in our work

Active ion	Faradic reaction	Theoretical capacitance (F/g)	Measured capacitance at 0.45V (F/g)	Utilization of cation
Ni^{2+}	$Ni^{2+} \leftrightarrow Ni^{3+} + e^{-}$	3646 (0.45 V)	10286 ($NiCl_2$)	282%
Ni^{2+}	$Ni^{2+} + 2e^{-} \leftrightarrow Ni$	7294 (0.45 V)		141%
Ni^{3+}	$Ni^{3+} + 3e^{-} \leftrightarrow Ni$	10941 (0.45 V)		94%

Theoretical specific capacitance of active cation $C_m = Q/(V \times M)$, where $Q = 9.632 \times 10^4$ C for transfer of 1 mol electrons, M is molecular weight of Ni ion (M = 58.693) and V is the operating voltage window.

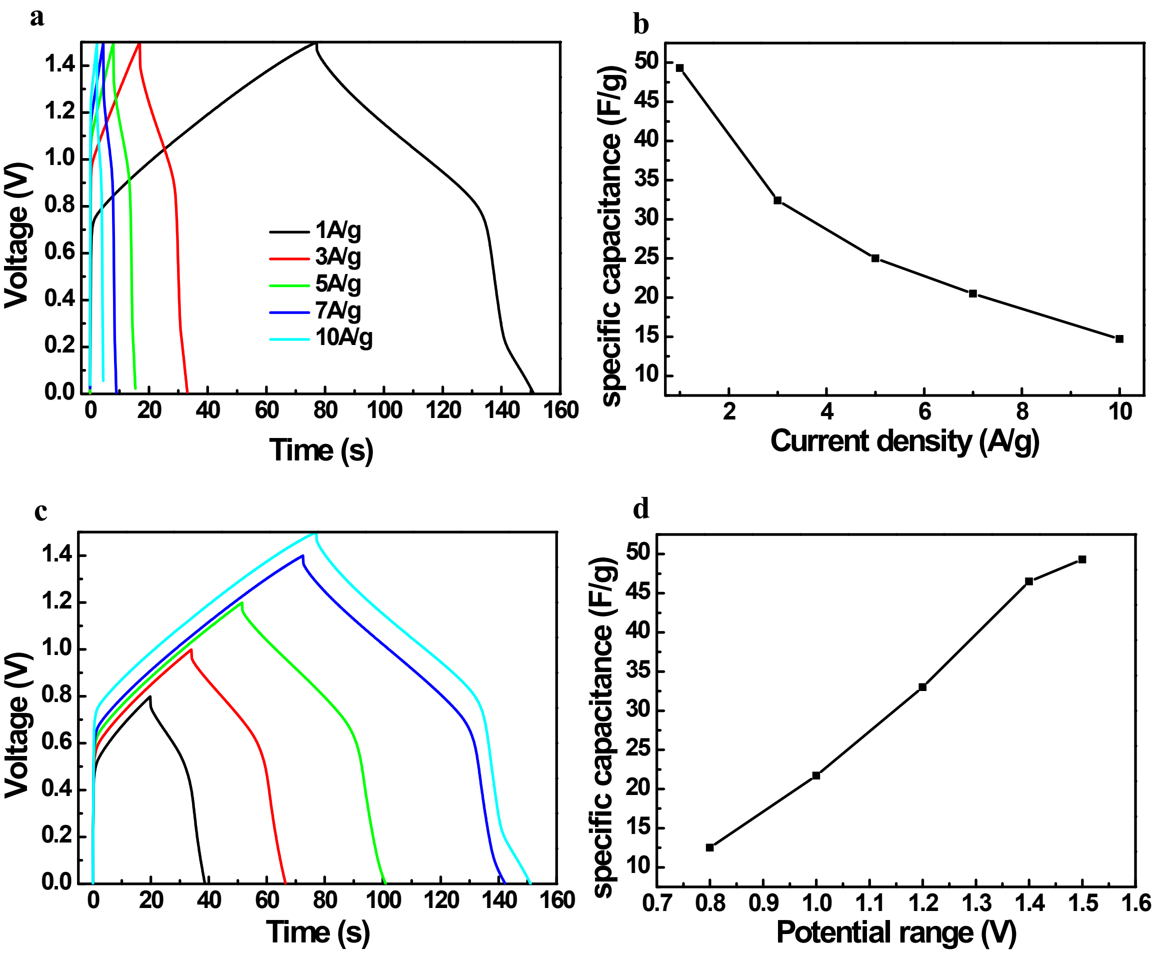

Figure S7 (a) The charge-discharge curves and (b) specific capacitance versus current density of asymmetric device. (c) The galvanostatic charge-discharge curves with different potential windows at the current density of 1 A/g. (d) Specific capacitance dependance on potential windows.